Research Square

Preprints are preliminary reports that have not undergone peer review.
They should not be considered conclusive, used to inform clinical practice,
or referenced by the media as validated information.

Molecular Interaction of *Candida albicans* with Polymeric Materials: Correlation of Single Cell Adhesion Forces, Gene Expression and Surface Characteristics

Saba Tamjidtash
Department of Prosthetic Dentistry and Biomedical Materials Science, Hannover Medical School, Hannover, Germany

Laura Brose
Department of Prosthetic Dentistry, UKR University Hospital Regensburg, Germany

Meike Stiesch
Department of Prosthetic Dentistry and Biomedical Materials Science, Hannover Medical School, Hannover, Germany

Katharina Doll-Nikutta
nikutta.katharina@mh-hannover.de

Department of Prosthetic Dentistry and Biomedical Materials Science, Hannover Medical School, Hannover, Germany

Sebastian Hahnel
Sebastian.Hahnel@klinik.uni-regensburg.de

Department of Prosthetic Dentistry, UKR University Hospital Regensburg, Germany

Nadine Kommerein
Department of Prosthetic Dentistry and Biomedical Materials Science, Hannover Medical School, Hannover, Germany

---

Research Article

Keywords: Candida albicans adhesion, atomic force microscopy, single-cell force spectroscopy, polyvinyl chloride, polytetrafluoroethylene, surface hydrophobicity

Posted Date: June 11th, 2026

DOI: https://doi.org/10.21203/rs.3.rs-9967429/v1

License: This work is licensed under a Creative Commons Attribution 4.0 International License.
Read Full License

Additional Declarations: The authors declare no competing interests.

Abstract

Candida albicans (*C. albicans*) is a commensal member of the oral microbiota capable of forming biofilms that may contribute to the development of denture stomatitis. The initial adhesion of the fungus to abiotic surfaces is a critical step in biofilm formation and is strongly influenced by the underlying material's physicochemical properties. Surface roughness, surface free energy (SFE), and salivary components, in particular, play a key role in mediating fungal-material interactions. Polymeric materials are essential components of denture materials, so understanding how they interact with *C. albicans* is crucial to clarifying the mechanisms underlying early fungal adhesion. However, the molecular and biophysical mechanisms that govern fungal adhesion to polymer materials are not well characterized. This study examined *C. albicans* adhesion behavior on polyvinyl chloride (PVC) and polytetrafluoroethylene (PTFE) surfaces with defined roughness levels (Ra = 0.2 µm and 0.04 µm) in the presence of artificial saliva. Surface properties were characterized using profilometry and contact angle measurements, while adhesion forces and cell–surface interactions were analyzed by single-cell force spectroscopy (SCFS) using atomic force microscopy (AFM) under varying contact forces and following saliva pretreatment. Additionally, the expression of the adhesion- and biofilm-associated genes *ALS1*, *HWP1*, and *EGP1* was quantified by quantitative reverse transcription PCR (qRT-PCR). Increased surface roughness resulted in stronger adhesion forces and an increased number of contact points. In contrast, higher surface free energy was associated with reduced adhesion. Saliva pretreatment further modulated these interactions. Gene expression analyses revealed that early adhesion is primarily regulated by polymer-dependent surface signals, while hyphae- and biofilm-specific pathways exhibited minimal activation. In summary, the results demonstrate that the surface properties of polymeric materials significantly influence the early adhesion of *C. albicans* and its associated molecular responses.

1 Introduction

Candida albicans (*C. albicans*) is a naturally occurring microorganism in the oral cavity and constitutes an integral part of the resident microbiota (1). This polymorphic fungus primarily exists in the yeast form (coccoid circular cells) but can transition into hyphal and pseudohyphal structures. Within the oral environment, *C. albicans* predominantly grows as biofilm, characterized by a surface attached, highly structured and dynamic three-dimensional organization with surrounding extracellular matrix (2–4). The strong adhesion properties of *C. albicans* enable it to also firmly attach to polymer-based denture materials, facilitating the development of denture stomatitis — a multifactorial inflammatory condition (5, 6). Biofilms are notably difficult to eradicate, posing a challenge in the treatment of Candida-associated stomatitis and often leading to persistent infections (3). Consequently, chronic inflammatory oral candidiasis affects up to 70% of denture wearers (7, 8). Furthermore, Candida infections are an increasingly important clinical problem, particularly in elderly and immunocompromised individuals, where they can lead to invasive candidiasis and even sepsis (9, 10).

The initial adhesion of yeast cells to surfaces within the first minutes of contact starts the pathogenic biofilm development of *C. albicans* (11). The process is mediated by several molecular mechanisms, including the expression of surface molecules such as adhesins (e.g., ALS1, ALS3, HWP1), which directly bind the cells onto the surface (12, 13). Therefore, they are considered virulence factors, which are often regulated in response to environmental cues, including surface contact and salivary components. A detailed understanding of the molecular and physicochemical mechanisms governing this adhesion process is essential for developing targeted anti-biofilm strategies. It has already been shown that the physicochemical properties of the underlying denture material — such as surface roughness, surface free energy (SFE), and chemical composition — significantly influence *C. albicans* adhesion dynamics (11, 18). For example, a previous study has demonstrated that both SFE and surface roughness are key determinants of fungal adhesion and biofilm formation on polymeric materials (11). In addition, biological fluids like saliva modulate these surface characteristics and may either enhance or inhibit fungal attachment (11). However, despite the growing recognition of surface-material interactions in microbial adherence, polymer-based materials remain comparatively understudied in the context of *C. albicans* biofilm formation (11). To date, only a limited number of studies have addressed the molecular mechanisms of *C. albicans* adhesion to polymeric materials particularly considering the role of artificial saliva and detailed surface characteristics (19–22). However, understanding the fundamental interactions between *C. albicans* and polymer substrates could guide the development of biomaterials optimized for medical and dental applications, ultimately leading to reduced infections and enhanced patient safety.

Over the past decade, atomic force microscopy (AFM) has emerged as a powerful tool for imaging microorganisms and analysing their mechanical behaviour at the nanonewton scale (23, 24). Recently, AFM and the related fluidic force microscopy (FluidFM) technique have proven effective in characterizing cell adhesion at both the single-cell and single-molecule level in a method called single cell force spectroscopy (SCFS) (25). FluidFM is a hybrid form of AFM and microfluidics that uses a cantilever with a microfluidic channel connected to a pressure control system to reversibly immobilize single cells on a probe tip, allowing detailed analysis of interactions between *C. albicans* and material surfaces in comparable high throughput (26, 27). This technology holds the potential to provide novel molecular insights into how surface properties, such as roughness and salivary conditioning, influence initial fungal adhesion. While AFM measurements reveal changes in mechanical properties and cell–material interactions at the nanoscale, RNA isolation followed by gene-specific quantitative real-time PCR (qRT-PCR) provides additional insights into underlying molecular biological processes, such as changes in gene expression. Combining both methods could therefore enable a more comprehensive understanding of molecular processes at the cell–material interface. In particular, integrating AFM with qRT-PCR may help directly link mechanical changes to cellular molecular responses, an approach that has so far been only sparsely or not yet systematically explored.

The aim of the present study was to investigate the molecular processes of *C. albicans* adhesion on two representative polymeric materials—polyvinyl chloride (PVC) and polytetrafluoroethylene (PTFE)—featuring defined surface roughness levels (rough vs. fine) and known differing hydrophobicity. To

investigate this interaction, the materials were characterized by profilometry and contact angle measurements to assess roughness and SFE, including its polar and dispersive components. Adhesion forces were measured using SCFS with FluidFM Different setpoint forces were applied to vary the contact force between the cell and the surface, and surfaces were pretreated with saliva to simulate more physiologically relevant conditions. In addition, the molecular expression of key virulence genes involved in adhesion and subsequent biofilm formation (*ALS1*, *HWP1* and *EGP1*) was analysed using qRT-PCR. Finally, surface properties and biological characteristics were mathematically correlated to identify central molecular responses of *C. albicans* to polymeric materials.

2 Materials and methods

2.1 Preparation and characterization of test specimens

2.1.1 Material preparation

The test specimens were made of polyvinyl chloride (PVC, PVC-U, Modulor, Berlin, Germany) and polytetrafluoroethylene (PTFE, online-plast, Koblenz, Germany). Cylindrical bars with a diameter of 20 mm were cut into 2 mm thick specimens (n = 10) using a precision cutting machine (Accutom-100, Struers, Willich, Germany) equipped with a diamond cut-off wheel (E0D15, Struers, Willich, Germany).

The specimens underwent an automated polishing process to ensure uniform and reproducible surface finish. This polishing process consisted of two sequential surface treatments designed to achieve distinct surface roughness levels: The initial rough treatment (intended R_a = 0.2 µm) was performed under water cooling using a silicon carbide (SiC) foil (#1000 grit, Struers, Willich, Germany). In the subsequent fine surface treatment (intended R_a = 0.04 µm), specimens were further polished under water cooling using a finer SiC foil (#2500 grit, Buehler, Düsseldorf, Germany) following the initial #1000 grit treatment.

For qualitative analysis of surface topography, one randomly selected specimen per group (n = 1) was examined using scanning electron microscopy (SEM; Phenom, FEI, Eindhoven, The Netherlands). Prior to imaging, specimens were thoroughly cleaned to remove potential dust particles and subsequently mounted on aluminium stubs. To minimize charging effects, a thin platinum layer was applied via sputter coating for 50 seconds. SEM imaging was then performed at the centre of each specimen using a top-down view at 1500× magnification.

The specimens were subjected to sterilisation before biological experiments through immersion in an alcohol-based disinfectant (Bacillol AF, Hartmann, Heidenheim, Germany) for approximately 5 minutes. Following the sterilisation process, three rinsing steps were conducted using sterile distilled water.

2.1.2 Quantitative analysis of surface roughness

To estimate surface roughness, measurements were conducted at the centre of each specimen and parallel to the grinding lines using a tactile contact profilometer (LT = 1.7 mm, LC = 0.25 mm, velocity 0.1 mm/s, Perthometer S6P, Perthen Mahr, Göttingen, Germany). The profilometer was equipped with a diamond stylus featuring a tip radius of 2 µm to measure the surface roughness, with a single measurement per specimen. The primary roughness parameters analysed were the arithmetic mean roughness (R_a) and the maximum roughness value (R_z), both representing two-dimensional line roughness characteristics.

2.1.3 Surface wettability via contact angle measurement

The surface free energy (SFE) was determined using the sessile drop method with two liquids of different surface tensions. Prior to measurement, polymer surfaces were cleaned with 70% ethanol. Contact angles were measured at 23°C using a computer-assisted goniometer (DSA25, Krüss, Hamburg, Germany). Droplets (4 µL) of deionized water and 99% diiodomethane (ReagentPlus, 99%, Merck KGaA, Darmstadt, Germany) were placed on the surface, and contact angles were measured on both sides of each droplet to assess surface hydrophilicity. The SFE was then calculated using the Owens and Wendt method (28).

Contact angle measurements under salivary conditions were performed using a device from DataPhysics Instruments GmbH, OCA 40 (Filderstadt, Germany). All specimens underwent the cleaning procedure described above. For saliva-coated specimens, samples were then incubated in artificial saliva (see below) at 37°C for 2 hours (to adapt to the experimental conditions), rinsed once with phosphate-buffered saline (PBS; Sigma-Aldrich Chemie GmbH, Taufkirchen, Germany) and air-dried at room temperature for 10–20 minutes. For control samples, specimens were immersed in deionized water for approximately 1 hour and subsequently air-dried at room temperature for 10–20 minutes. For both conditions, two specimens per material were examined, with five measurements per deionized water and diiodomethane performed on each specimen (n = 10 per liquid and material, including technical replicates). Measurements were conducted using 5 µL droplets of the aforementioned liquids.

2.2 Microbiological experiments

2.2.1 Yeast strain and growth conditions

The yeast strain *Candida albicans* DSM 1386, sourced from the German Collection of Microorganisms and Cell Cultures (DSMZ, Braunschweig, Germany), was preserved at -80°C in glycerol stocks. Cultivation was carried out in liquid 186 medium, prepared according to the DSMZ's guidelines, excluding agar. The medium included 3 g/L yeast extract, 3 g/L malt extract, 5 g/L soybean-derived peptone, and 10 g/L glucose monohydrate (all Carl Roth GmbH & Co. KG, Karlsruhe, Germany). For the pre-culture stage, the *C. albicans* strain was incubated for 24 hours at 30°C with continuous agitation at 200 rpm.

2.2.2 Preparing artificial saliva

Artificial saliva was prepared according to previously described protocols (29–33) using the following components: 8.5 mg/mL mucin from porcine stomach, 1 mg/mL lysozyme from chicken egg white, 100 mg/mL α-amylase from hog pancreas, and 4 mg/mL bovine serum albumin (BSA), all obtained from Sigma-Aldrich (Taufkirchen, Germany). Each component was diluted at a 1:100 ratio in PBS (29–33).

Sterilization was carried out as follows: mucin and α-amylase solutions were autoclaved, while the BSA and lysozyme solutions were sterilized by filtration through a 0.22 µm membrane. To confirm sterility of the artificial saliva, the solution was incubated in a 6-well plate (Greiner Bio-One, Frickenhausen, Germany) with two different media: 15 g/L tryptone soya broth (Oxoid, Basingstoke, Hampshire, UK) and 186 medium. The incubation was carried out at 37°C for 24 hours. The saliva was considered sterile if there were no macroscopic signs of contamination; that is, if the media looked the same as the control medium without saliva. The saliva was then used for experiments.

For saliva experiments, the test specimens were incubated with freshly prepared artificial saliva at 37°C for 2 hours. Following incubation, saliva was removed, and the specimens were rinsed once with PBS.

2.2.4 Preparation of yeast test suspension

Following centrifugation (10 minutes at 4000 rpm), the supernatant of the pre-culture was discarded. Subsequently, two washing steps were conducted with 50 mM Tris-HCl. For this purpose, Tris(hydroxymethyl)aminomethane (Tris, Carl Roth GmbH & Co. KG, Karlsruhe, Germany) was dissolved in deionized water, and the pH was adjusted to 7.5 using 37% hydrochloric acid (HCl, Carl Roth GmbH & Co. KG, Karlsruhe, Germany). After each washing step, the cells were harvested by centrifugation under identical conditions. After the second washing step, the resulting pellet was resuspended in PBS. The cell suspension was adjusted to an optical density of 1.0 at 600 nm and diluted 500-fold in PBS.

2.2.5 Single-cell force spectroscopy (SCFS)

All SCFS experiments were conducted in PBS at room temperature, using a FlexFPM atomic force microscope (Nanosurf GmbH, Liestal, Switzerland) equipped with a FluidFM module, mounted on an inverted microscope (Eclipse Ti-S, Nikon GmbH, Düsseldorf, Germany) as described in Doll-Nikutta et al. (34). Tipless FluidFM micropipettes (Cytosurge AG, Glattbrug, Switzerland) with a nominal spring constant of 0.3 N/m and an aperture of 2 µm were used for the measurements. The spring constant of each cantilever was determined through thermal tuning, using scripts implemented in the software, with values ranging from 0.29 to 0.61 N/m. During the experiment, the optical focus was set to 60x magnification. The test specimens were placed in a Petri dish (WillCo Wells B.V., Amsterdam, The Netherlands) using a glass ring with an off-center opening, which was designed to have material and cells on the same level (**Figure S1**). The setup was subsequently inoculated with the freshly prepared cell suspension.

To capture *C. albicans* on the glass surface, the cantilever was microscopically focused on a single cell. The cantilever was then approached to the cell with a setpoint of 5 nN at a speed of 2 µm/s, followed by a 5-second pause with vacuum of -400 mbar and a subsequent retraction of 7 µm. After verifying

successful capturing microscopically, the cantilever transported the cell across the material surface for force spectroscopy. For each adhesion force measurement, the captured cell was brought in contact with surface for an adhesion time of 2 seconds with a setpoint force of 0.75 nN or 10 nN. A total of 16 force spectroscopy curves were recorded for each cell at different positions within a 10x10 µm area.

The analysis of the force-distance curves was performed using the program established by Doll-Nikutta et al. (34). The curves were meticulously examined and subjected to a rigorous quality control process to eliminate any erroneous data and ensure that they represented conditions devoid of surface contact. By this, a total of 63 to 201 individual force measurements could be included in further analysis, depending on the condition. Subsequent calculations were executed using the MATLAB R2023a software to analysed the parameters attachment points, maximum adhesion force, and detachment distance as shown in Fig. 1.

2.2.6 Gene expression analysis

Candida albicans biofilm formation

To obtain sufficient amounts of genetic material, *C. albicans* was grown as biofilm on the test specimens. As described above, the yeast was pre-cultured in 186 medium and adjusted to an OD600 of 0.1 in the same medium. The suspension was inoculated onto the samples mounted in 6-well plates (Greiner Bio-One) and incubated for 24 hours at 37°C under 5% CO_2 atmosphere. Plates without test specimens served as control surfaces. After incubation, the medium was removed and the samples were washed twice with PBS.

To assure successful cultivation, biofilms were stained with the dyes SYTO 9 and propidium iodide (Live/Dead BacLight Bacterial Viability Kit, Thermo Fisher Scientific, Waltham, MA, USA) according to the manufacturer's protocol for 30 minutes, followed by a PBS wash. The biofilms were then fixed with 2.5% glutaraldehyde (Carl Roth GmbH + Co. KG, Karlsruhe, Germany) for 15 minutes. Confocal laser scanning microscopy (CLSM; Leica TCS SP8, Leica Microsystems, Mannheim, Germany) at 63x magnification was used to acquire image stacks of the biofilms. SYTO9 was excited at 488 nm (emission 500–550 nm) and propidium iodide at 552 nm (emission 675–750 nm), with five stacks captured per specimen and control using a 1 µm z-step. Surface coverage (area fraction, %) was evaluated using ImageJ (35). To quantify biofilm height distribution, image stacks were processed using Imaris X64 8.4.2 (Bitplane AG, Zurich, Switzerland) to first yield the total biofilm volume (µm³). Then, biofilm height distribution was obtained by dividing the total biofilm volume (µm³) by the projected total area (µm²).

Extraction and purification of RNA

RNA was extracted from 10 specimens with *C. albicans* biofilms per condition. After removal of the medium, specimens and control wells were washed with PBS, and biofilms were mechanically detached, pooled, and pelleted by centrifugation (16,000 ×g, 10 minutes, 4°C). Cell pellets were resuspended in lysis buffer and total RNA was isolated using the Quick-RNA Fungal/Bacterial Microprep Kit (Zymo

Research, California, USA) according to the manufacturer's instructions, including mechanical disruption with bead beating. For this purpose, the samples were homogenized for 10 minutes using a Vortex-Genie 2 (Scientific Industries, Bohemia, NY, USA) at speed setting 6 with a tube-holder attachment. On-column DNase I treatment was performed by mixing 5 µL DNase I (Cat. No. E1011-A, Zymo Research Corp.) with 35 µL of DNA digestion buffer, applying the mixture to the ethanol-washed column, and incubating for 15 minutes at room temperature. The RNA was eluted in RNase-free water, and concentration and purity were assessed spectrophotometrically (NanoDrop 2000, Thermo Fisher Scientific, Erlangen, Germany). The RNA samples were adjusted to 100 ng/µl and either used immediately for cDNA synthesis or stored at − 80°C until further use.

Reverse transcription of RNA to cDNA

Total RNA was reverse transcribed into cDNA using the QuantiTect Reverse Transcription Kit (Qiagen, Hilden, Germany) according to the manufacturer's instructions. Genomic DNA was eliminated by incubating 1 µL of diluted RNA with 2 µL of gDNA Wipeout buffer and 11 µL of RNase-free water for 2 minutes at 42°C. The reverse transcription reaction (20 µL total) was assembled by combining 14 µL of the treated RNA with 1 µL of QuantiScript Reverse Transcriptase, 4 µL of 5× RT buffer, and 1 µL of RT Primer Mix. It was incubated for 15 minutes at 42°C and 3 minutes at 95°C to inactivate the enzyme. No-RT controls were included to exclude genomic DNA contamination. cDNA samples were either used immediately for quantitative real-time PCR (qRT-PCR) or stored at − 20°C until analysis.

Real-time PCR to quantify Candida virulence genes

Quantitative real-time PCR (qRT-PCR) was performed using SYBR Green chemistry (iQ SYBR Green Supermix, Bio-Rad, California, USA). Gene expression levels of *ALS1*, *HWP1*, and *EFG1* were analyzed using *ACT1* as the reference gene. Primers (Table 1) were obtained from Eurogentec (Seraing, Belgium). Reactions were performed in technical duplicates, including no-template and no-RT controls, on a Bio-Rad iQ5 Real-Time PCR Detection System (Bio-Rad Laboratories). Cycling conditions are summarized in Table 2. Following PCR, the data were expressed as ΔCt values, calculated by subtracting the Ct of the reference gene ACT1 from that of the target genes. To improve comparability, the ΔCt values were normalized to the control well and presented as percentages.

Table 1
Primers used for qRT-PCR analysis, including sequence (5'–3'), length (bp) and GC content (%).

Gene	Primer	Sequence (5’–3’)	Length (bp)	GC content (%)
ACT1	Forward	GACCGAAGCTCCAATGAATC	20	50
	Reverse	AATTGGGACAACGTGGGTAA	20	45
ALS1	Forward	AGAACTGATTTGCAGTGATGG	21	42.9
	Reverse	TGAGGATTCATTGCTATCTGG	21	42.9
EFG1	Forward	TATCACGTGAATATTTCCAGGG	22	40.9
	Reverse	CTGACTGTTCGTTGTGATTTGG	22	45.5
HWP1	Forward	GACCGTCTACCTGTGGGACAGT	22	59.1
	Reverse	GCTCAACTTATTGCTATCGCTTATTACA	28	35.7

Table 2
PCR cycling conditions (36).

Step	Temperature (°C)	Time
Initial denaturation	95	10 minutes
Denaturation	95	20 s
Annealing	54	20 s
Extension	72	30 s
Cycles		40×
Final step	75	3 minutes

2.3 Statistical analysis and linear correlation

Statistical analyses were performed using GraphPad Prism version 10 (GraphPad Software Inc., La Jolla, CA, USA). The level of significance was set at $\alpha = 0.05$. Surface parameters of the untreated standard polymers (R_z, Ra, SFE, and the polar and dispersive components) and results of gene expression were analyzed using the Kruskal–Wallis test due to non-normal data distribution identified by Shapiro-Wilk test, followed by Dunn’s multiple comparison test. Surface parameters after saliva treatment (contact angle, SFE, polarity, and dispersive components) and SCFS results (maximum adhesion force, number of adhesion points, and detachment distance) were evaluated by two-way ANOVA to assess the effects of material and saliva or material and measurement condition, respectively, followed by Tukey’s post hoc test.

The correlation between surface parameters and microbiological results was analyzed using simple linear regression. First, individual values were normalized relative to the 0.2 µm surface value, and then

the regression line was plotted with a 95% confidence interval. Additionally, R^2, the correlation coefficient indicating the quality of the model fit to the data, was reported.

3 Results

3.1 Polymeric surface characterization

The surface properties of PVC and PTFE, subjected to two distinct surface treatments (0.2 µm: rough; 0.04 µm: fine), were analysed in terms of surface roughness and wettability. In general, both materials exhibited a more homogeneous and smoother surface morphology following the fine treatment compared to the rough treatment as visible by SEM (Fig. 2a).

The roughness measurement (R_a and R_z) in Table 3 verified the efficacy of the treatments in creating uniform surfaces across different materials. Both treatments resulted in arithmetic average roughness R_a values close to the aspired 0.2 µm, respectively 0.04 µm, for both materials. For the maximum peak to valley height, R_z, PTFE achieved slightly but not significantly higher roughness values than PVC for both treatments.

The SFE was determined based on contact angle measurements, including their dispersive and polar components (Fig. 2b**)**.

With regard to the SFE, a pronounced influence of both material properties and surface treatment was observed. Fine treatment resulted in increased SFE, whereas rough treatment tended to yield lower values. Specifically, PTFE exhibited significantly lower SFE values than PVC after rough treatment. After fine treatment, the SFE increased by more than 5 mJ/m² for both PVC and PTFE. The finely treated PVC surface showed the highest SFE values overall.

The dispersive component of the SFE followed a comparable trend, with PTFE displaying significantly lower values than PVC. Fine treatment led to an increase in the dispersive component for PVC and PTFE.

By contrast, the polar components of the SFE were comparable across most samples. However, an exception was observed for finely treated PTFE, which exhibited a significantly elevated polar component. Overall, the polar components were approximately 30-fold lower than the dispersive components.

Table 3
Mean values and standard deviations (SD) of the roughness parameter R_a and R_z Identical letters show significant differences between the indicated materials and treatments ($p \leq 0.05$).

material	roughness parameter	
	R_a (µm)	R_z (µm)
PVC (0.2 µm)	0.21 (0.01) [a]	1.47 (0.07) [b]
PVC (0.04 µm)	0.05 (0.01) [a]	0.51 (0.02) [b]
PTFE (0.2 µm)	0.23 (0.01) [c]	1.63 (0.07) [d]
PTFE (0.04 µm)	0.05 (0.01) [c]	0.54 (0.02) [d]

3.3 Influence of saliva treatment on polymer surfaces

The effect of saliva on wettability was assessed by contact angle measurements as well. To ensure comparability, control samples were pretreated with water instead of saliva, dried, and subsequently analysed. The resulting wettability, SFE and its dispersive and polar components are shown in Fig. 2. Prior to salivary conditioning, all materials and surface treatments exhibited comparable static water contact angles. No significant differences were observed between the roughness levels for either material. After salivary conditioning, PVC surfaces exhibited a decrease in contact angle for both roughness levels, indicating enhanced surface hydrophilicity. In contrast, PTFE surfaces showed no statistically significant changes following saliva exposure. However, a slight reduction in contact angle was noted for the 0.04 µm PTFE surface, suggesting a minor increase in wettability.

Figure 2c illustrates the SFE values calculated based on the contact angles of water and diiodomethane. For the control treatment, no statistically significant differences in SFE were observed between PVC and PTFE surfaces, regardless of the roughness. Under all conditions, the mean SFE was approximately 25 mJ/m². This contrasts with the wettability of untreated surfaces, where significant material-dependent differences could be detected. Following saliva conditioning, the SFE of PVC surfaces increased significantly by about 20 mJ/m² compared to unconditioned PVC. PVC also showed significantly higher SFE than PTFE of the same roughness. For PTFE at 0.2 µm, a small but significant increase in SFE was observed after saliva adsorption, whereas no significant change occurred for PTFE at 0.04 µm.

The dispersive components of the SFE show that, after the water control treatment, there were no significant differences in either PVC or PTFE, irrespective of roughness, and the values remained below 20 mJ/m². This differs from the untreated surfaces, where material-dependent differences were evident. Saliva coating produced a similar pattern across all samples, with no significant differences between materials. It caused a significant increase in the dispersive component except for smooth PTFE. Here, no

statistically significant change was detected, although a slight tendency toward higher dispersive values was noted.

The polar components of the SFE, as shown again, demonstrated that the polar contributions remained largely unchanged across all materials and roughness levels after the control treatment. Following saliva conditioning, PVC surfaces exhibited an almost two-fold increase in polar components regardless of the roughness. In contrast, saliva coating did not alter the polar components of PTFE surfaces, which were then significantly lower than those of the corresponding PVC surfaces.

3.4 Adhesion forces of *Candida albicans* on polymer surfaces at different contact pressures

To investigate the initial biophysical adhesion process of *C. albicans* on polymer surfaces, reversible adhesion forces of individual cells were examined after two seconds adhesion time using FluidFM-based SCFS under varying contact forces. Representative force-distance curves are shown in Fig. 3a. Three parameters were quantified from these curves: maximum adhesion force, number of adhesion points, and detachment distance (Fig. 1).

Maximum adhesion force, defined as the peak force required to detach a cell from the surface, is mainly determined by non-specific Lifshitz–van der Waals and electrostatic interactions (37). The analysis showed that the maximum adhesion force depended on an interaction between material properties, surface roughness, and contact force. Overall, forces tended to decrease with increasing contact force. At low contact force (0.75 nN), the material effect dominated: adhesion forces on PTFE were significantly higher than on PVC, regardless of the roughness. This pattern reversed at higher contact forces (10 nN), with PVC exhibiting significantly higher adhesion forces than PTFE. In addition, a significant roughness effect was observed: rougher PVC surfaces significantly increased adhesion at higher contact forces. A comparable effect was not observed on the other surfaces.

The number of adhesion points reflects the number of specific interactions (e.g., hydrogen bonds) between cell surface molecules and the tested surface (38, 39). The results were similar to those for maximum adhesion force, but somewhat more pronounced. At low contact pressure, significantly more adhesion points were observed on PTFE than on PVC. However, this effect was limited to rough surfaces. As contact pressure increased, the trend reversed, with more adhesion points observed on PVC than on PTFE, but again only on rough surfaces. Overall, the number of adhesion points decreased markedly for PTFE, while increasing only slightly for PVC. At higher contact pressure, significant roughness effects were observed for PTFE: smooth surfaces showed significantly fewer adhesion points than rougher surfaces.

Detachment distance reflects the length and flexibility of surface-bound molecules and the cell membrane, which stretches during detachment (40, 41). In general, increased contact force on smooth surfaces of both materials resulted in longer release distances. At a contact force of 0.75 nN, no

significant differences were observed between the materials or roughness levels. Even under higher loads (10 nN), no material effect was detected. However, release distances on smooth PTFE surfaces were significantly longer than on rough PTFE surfaces.

3.5 Influence of saliva on the adhesive forces of *Candida albicans*

After examining the effect of different contact forces, the influence of artificial saliva on *C. albicans* adhesion forces on PVC and PTFE surfaces was analyzed by SCFS. The contact force was kept constant at 10 nN and the results were compared with the previous values obtained without saliva. This contact force was chosen based on preliminary tests: lower forces in the presence of saliva produced unstable, non-reproducible force curves that could not be stabilized even by extending adhesion time. The higher contact force, however, yielded reproducible and evaluable data. Exemplary force-distance curves are shown in Fig. 3b.

The results showed that saliva significantly altered the initial adhesion behavior of *C. albicans*. While the maximum adhesion force without saliva differed little between materials, it increased significantly on almost all tested surfaces after saliva conditioning (except PVC 0.04 µm). The effect varied by material: PTFE surfaces consistently showed higher adhesion forces than PVC, with no roughness dependency. In contrast, only rough PVC surfaces showed significantly higher adhesion forces, while adhesion forces on smooth PVC remained low. Overall, saliva mainly increased absolute adhesion force but also changed the relative influence of material properties and roughness, making these factors more pronounced.

The number of adhesion points was similarly affected by saliva and again depended on material and roughness. Without saliva, adhesion points followed the same pattern as maximum adhesion force, with more adhesion points on PVC and fewer on smoother surfaces of both materials. With saliva, adhesion points on rough PVC decreased significantly but remained higher than on rough PTFE. On smooth surfaces, the opposite occurred: adhesion points on PVC decreased while those on PTFE increased significantly, so that PTFE now showed more adhesion points. Within PTFE, adhesion points became similar across roughness levels, whereas PVC showed a clear dependence: smooth surfaces had significantly fewer adhesion points than rough ones. In summary, saliva reduced adhesion points on PVC, while increasing them on smooth PTFE, again indicating that saliva changes the hierarchy of influencing factors and accentuates material-dependent differences.

Detachment distance was influenced by both roughness and saliva. Without saliva, both materials showed significant roughness effects with longer release distances on smoother surfaces. After saliva coating, this pattern reversed for PVC, while PTFE showed no difference. Values on PTFE and smooth PVC were comparable, while only rough PVC exhibited a significantly higher release distance.

3.8 Influence of standard polymer surfaces on gene expression in *Candida albicans* biofilms

After systematically investigating *C. albicans* adhesion at the surface molecule level, the influence of surface properties of polymers was also examined at the molecular level. The focus was on three target genes—*ALS1*, *HWP1*, and *EFG1*—with *ACT1* used as a housekeeping gene for normalization.

To obtain sufficient amounts of RNA, gene expression was analyzed in *C. albicans* biofilms. Their successful formation was verified by confocal laser scanning microscopy after 24 h of cultivation (Fig. 4a: representative CLSM images). Figure 4b shows the relative surface coverage of the biofilms formed on the four different surfaces. When comparing the two material types, PTFE surfaces had significantly higher surface coverages than PVC surfaces, regardless of the surface treatment applied. Within each material, differences in roughness did not lead to differences in surface coverage. While PVC 0.2 µm even had a lower median surface coverage than PVC 0.04 µm, this difference was not statistically significant. This indicates that material composition has a more pronounced effect on biofilm formation than the specific surface treatment used.

Figure 4b also shows the distribution of biofilm height on the different materials, which appeared as opposite picture compared to surface coverage. PVC 0.2 µm exhibited the highest biofilm height among all tested surfaces, being significantly higher compared to PVC 0.04 µm and PTFE 0.2 µm. In contrast, PTFE 0.2 µm and PTFE 0.04 µm showed no significant differences in biofilm height between them and demonstrated generally lower height values compared to the PVC surfaces.

The results verified successful biofilm formation and demonstrated a clear material-dependent pattern in both surface coverage and biofilm height. The findings suggest that PTFE favors broad but thin biofilm formation, whereas PVC promotes more vertical accumulation, despite lower overall coverage.

For gene expression analysis, biofilms from ten identical test specimens were pooled, RNA was extracted, and cDNA was synthesized. Gene expression was analysed by qRT-PCR using SYBR Green. Figure 4c shows the resulting ΔCt values, calculated by subtracting the Ct value of the housekeeping gene *ACT1* from that of each target gene. For comparability, values were normalized to the control surface (well plate) and presented as percentages.

The results showed that *ALS1* was expressed most strongly, followed by *HWP1*. *EFG1*, a master regulator of morphogenesis and biofilm formation, was barely detectable or undetectable and could not be reliably amplified on either the control surface or the polymer materials. With Ct values > 35, some data points even fell below the detection limit. This indicates very low or no expression, so the results should be interpreted with caution. A change in expression on smoother surfaces is possible but would require further experiments to confirm.

The Ct values for *ALS1*, an adhesin, were lower on all polymer surfaces than on the control, indicating higher transcript levels (lower Ct/ΔCt values correspond to higher expression). This increase was most pronounced on the 0.2 µm PVC and 0.04 µm PTFE surfaces, with expression approximately 20% higher than on the control. For PTFE 0.04 µm, the difference was statistically significant.

In contrast, *HWP1*, which is crucial for hyphal morphogenesis, showed consistently higher ΔCt values on polymer surfaces compared to the control. Higher ΔCt values indicate later amplification and, thus, a lower initial amount of *HWP1* transcripts, suggesting reduced expression of this hyphae-associated gene and limited hyphae formation on the polymer surfaces. For PVC 0.04 µm, this difference was statistically significant.

In summary, molecular analysis of virulence gene transcription showed that the surface properties differentially influence gene expression of adhesion and hyphae formation genes in *C. albicans*. While *ALS1* responded with a tendency toward increased expression, *HWP1* tended to be suppressed on polymeric materials

3.6 Linear correlation of surface parameters and molecular *Candida albicans* response

To identify overarching correlations that went beyond the individual effects already described for each material, a systematic correlation analysis of distinct parameter pairs was conducted. Prior to statistical evaluation, all data were normalized by setting the values of the finer surfaces (0.04 µm) in relation to the corresponding values of the rough surface (0.2 µm). This procedure enables a comparable evaluation of the surface effects, independent of absolute measurement fluctuations, and allows a differentiated analysis of the influence of individual surface parameters.

The results of the correlation analysis of material characteristics, adhesion forces and gene expression are shown in Fig. 5. Overall, the data showed a heterogeneous pattern. A clear correlation could be observed between surface roughness and all three adhesion force parameters. The maximum adhesion force, the number of adhesion points and the detachment distance all correlate positively with the Ra values of the surfaces. Additionally, a correlation was demonstrated between the attachment points, the detachment distance and the SFE. Conversely, the correlation between the maximum adhesion force and the SFE was only moderate. An additional isolated correlation was found between surface polarity and detachment distance.

Correlation analysis of the qRT-PCR data with surface parameters revealed moderate overall associations. *ALS1* expression correlated positively with surface roughness, while surface polarity showed a moderately negative correlation with *HWP1* and *EFG1* expression.

In order to additionally include the influence of saliva on this interaction, the respective results with saliva were normalized to the results without saliva. The relative adhesion forces with saliva were then linearly correlated again with the surface wettability parameters. Thus, the results in Fig. 6 show whether saliva caused a systematic change in the interaction between the parameters examined.

It could be detected that the changes in maximum adhesive force and in the polar components of the surface after saliva conditioning showed a moderate correlation. To a slightly lesser extent, the change

in the number of adhesion points was also linked to polarity. Conversely, the release distance showed a moderate correlation with the change in SFE after saliva conditioning.

4 Discussion

Adhesion to polymeric surfaces is the first and decisive step in the pathogenesis of *C. albicans* that can lead to infectious disease, such as denture-associated stomatitis. This biophysical process is governed by cell surface molecules and in turn influences gene expression, which causes the onset of pathogenic biofilm formation. To develop materials that reduce *C. albicans* denture colonization, knowledge on these molecular interactions in correlation to polymer surface properties is indispensable.

For this purpose, adhesion forces and virulence gene expression of *C. albicans* were investigated on two standard polymers (PVC and PTFE) with known differences in wettability and two roughness levels, each. The influence of saliva conditioning was additionally analyzed. Surface parameters had a measurable impact on both adhesion forces and gene expression of *C. albicans*. Lower Roughness and higher SFE reduced the maximum adhesion force and the number of attachment sites, while decreasing roughness also moderately decreased the expression of the adhesion protein *ALS1*. In addition, low surface polarity moderately reduced the detachment distance but slightly increased the expression of the hyphal regulator *HWP1* as well as the biofilm promoting molecule *EFG1*.

Influence of material chemistry, treatment and artificial saliva coating on surface properties

The adhesion of *C. albicans* is influenced by a material's intrinsic surface properties such as roughness, wettability and SFE (42). The physicochemical surface properties of PVC and PTFE differ substantially, particularly with regard to wettability and surface free energy – which are known to influence microbial adhesion. The materials underwent surface treatments to achieve two defined roughness values. The roughness of Ra = 0.2 µm is considered the threshold for microbial colonization. The roughness of Ra = 0.04 µm corresponds to a significantly smoother surface that is expected to have minimal influence on microbial adhesion. Roughness measurements confirmed that these target values were achieved. Whilst the surface roughness of PVC and PTFE was specifically adjusted through surface treatment, the significant differences observed in their SFE are largely determined by the material's intrinsic chemical properties. Due to their more polar, hydrophilic surface, the PVC samples exhibited higher SFE values than the highly hydrophobic PTFE with significantly lower polar components.

Additionally, the material surface properties can also be used to indicate how saliva can alter a surface's wettability (43). The characterization of the investigated polymer surfaces showed that the coating with artificial saliva led to measurable changes in surface properties. A significantly reduced static water contact angle was observed on PVC surfaces after saliva application, which indicates increased wettability and, thus, an increase in SFE (44). These changes can presumably be attributed to the formation of an "acquired pellicle" (45), a thin adsorption layer of salivary proteins such as mucins, lysozymes or amylases, which create a more hydrophilic surface. The formation of this protein adsorption layer can modify the original surface chemistry by exposing hydrophilic functional groups

(e.g. -OH, -COOH) that can interact with water molecules via hydrogen bonds. This contributes significantly to increased wettability as demonstrated, for example, in a study in which both coated and uncoated titanium surfaces showed a significant reduction in the contact angle and, thus, increased hydrophilicity after saliva treatment (48). However, this effect could not be applied to all materials. On hydrophobic and chemically inert substrates such as PTFE, only a slight, non-significant reduction in contact angle was observed. This indicates that the adsorption of saliva proteins on highly hydrophobic surfaces is not sufficient to substantially change their low wettability, probably due to limited interaction partners. The intrinsically low surface energy of PTFE was, thus, largely retained despite the saliva coating.

Adhesion Forces of Candida albicans to polymeric surfaces

The adhesion forces of *C. albicans* to polymer surfaces were measured at the single cell level using fluidic force spectroscopy.

A decisive parameter in this measurement method is the setpoint force, i.e., the force exerted on the cell when it reaches the surface. The setpoint force is positively correlated with the measured adhesion forces and plays a central role in cell contact with the surface (49). Two different setpoint values were used in this study: 0.75 nN and 10 nN. In previous studies, similarly set points of 0.5–10 nN were used to investigate *C. albicans* adhesion strength (50–54). The lower value (0.75 nN) was chosen to avoid cell deformation while ensuring reliable contact between the cell and the surface. This value has already been proven to be suitable for bacterial measurement in previous studies (38, 40). An increased setpoint force of 10 nN was applied to allow for measurement on the saliva coated test specimens. Measurement in the presence of saliva was not possible with lower setpoint forces (e.g. 0.75 nN), as a stable cell contact could not be achieved under these conditions in preliminary experiments.

Another central parameter for adhesion force measurement is the adhesion time, i.e., the duration in which the cell remains in contact with the surface before the retraction movement is initiated. In the present study, the defined adhesion time was 2 seconds, which is in agreement with previous studies on *C. albicans* adhesion forces (3, 50, 52–54). It has been shown that microbial cells can already show measurable adhesion forces immediately after the first surface contact (49, 55, 56) with results for *C. albicans* already at zero seconds adhesion time (3). In general, longer adhesion times lead to increased adhesion strength due to the removal of interfacial water and subsequent stabilisation of cell–surface binding (49, 55, 57).

From the resulting force-distance curves, three central parameters for characterizing cell adhesion were recorded as part of this study: (1) the maximum adhesion force, which is primarily influenced by non-specific physicochemical interactions of the cell membrane, such as Lifshitz-Van der Waals and electrostatic forces (37, 39, 58); (2) the number of individual binding points that indicate specific interactions between cell surface molecules and the material surface (39, 55, 58); and (3) the distance of detachment, which describes the spatial expansion and mechanical flexibility of the molecules involved and, to a lesser extent, also reflects the deformability of the cell itself (37, 40, 50, 59).

All adhesion parameters showed variations depending on the material and the surface treatment. This was verified by correlation analysis: a linear correlation between roughness, SFE and adhesion forces could be detected. This applied to both the maximum adhesion force and the number of adhesion points, while the detachment distance also correlated moderately with polarity. The initial biophysical adhesion of *C. albicans* was, thus, determined by the interaction of surface chemistry and microstructure, which could be further supported by differences observed at the different set point forces. Force-dependent behavior can probably be explained by amyloid-like Als nanodomains, whose conformational changes under mechanical stress release high-affinity binding sites and most probably reacting differently to the underlying surface properties (60, 61).

At low contact forces, chemical-physical properties dominated, so that PTFE showed higher adhesion and more binding points than PVC. On highly hydrophobic substrates such as PTFE, hydrophobic interactions play a crucial role, mediated by the tandem repeat domains of Als proteins (62). Similar mechanisms have been described for *Candida glabrata* (Epa6 protein) (62). Likewise, studies on *Staphylococcus aureus* showed that hydrophobic surfaces adsorb many weakly binding macromolecules, resulting in high adhesion forces, while hydrophilic surfaces limit adhesion to a few strong binding sites (63). The hydrophilicity of polymer surfaces depends heavily on polar groups (-OH, -COOH, and chlorine), which can form hydration shells and act as barriers (64). However, under high mechanical stress, hydrophilic surfaces can develop stronger adhesive forces, possibly through additional hydrogen bonds and altered protein distribution (65).

With increasing force, roughness became more important: particularly rough PVC surfaces led to stronger adhesion forces and longer detachment distances, while smooth surfaces tended to shorter detachment distances. This shifted the adhesion behavior from material-dominated to roughness-influenced. Several studies confirm the importance of roughness for cell adhesion, as rough surfaces provide a larger contact area (66, 67). Overall, both cell wall ligands and polar and non-polar substrate groups mediate specific and nonspecific interactions. SFE controls chemical bonding, and roughness controls physical adhesion (68).

The saliva coating increased the adhesion forces on both polymers, but in detail depended on the material and roughness: Coated PTFE generally showed higher adhesion independently of roughness, while roughness was decisive for coated PVC with higher forces, more adhesion points and longer release distances on rough surfaces. Correlation analysis showed that under the influence of saliva the maximum adhesion force and to a certain extend the number of adhesion points was related to saliva-dependent changes in polarity, while changes in SFE correlated moderately with the detachment distance. Previous studies suggest that the initial adhesion of *C. albicans* is controlled by the binding of cell wall adhesins to the saliva layer (3). Saliva conditioning masks the material surface, so that chemical differences have less influence. Under high contact pressure, saliva could enhance the activation of mechanosensitive adhesion molecules, especially on hydrophobic surfaces such as PTFE, resulting in more stable bonds and higher adhesion forces. Overall, it appears that after saliva coating, interaction primarily occurs with the adsorbed saliva layer, which can form a strongly adhesive but short-

range matrix on smooth surfaces. Consequently, adhesion forces are more dependent of the surface's capability of saliva attraction than on the surfaces themselves.

These results highlight the complex interplay between material properties, surface chemistry, and biological factors in the adhesion of *C. albicans*. Initial adhesion is force-dependent and is determined by the combined effects of surface roughness, SFE, and polarity. Conditioning by saliva alters the influence of material chemistry. Overall, SFE and polarity seem to primarily control chemical bonding, while surface roughness determines the force-dependent stabilization of cell adhesion.

Influence of polymer surfaces on Candida albicans gene expression

The adhesion of *C. albicans* to a surface can be sensed intracellularly by the yeast and results in the adaption of gene expression. This leads to the onset of biofilm formation, for example. The analysis of biofilm formation and gene expression patterns of *C. albicans* on the different polymeric surfaces showed that the materials influenced the expression of adhesion- and morphogenesis-associated genes (*ALS1*, *HWP1*, *EFG1*). In particular, *ALS1* was sensitive to certain surfaces, with a tendency towards upregulation, while *HWP1* tended to be downregulated. In contrast, *EFG1* showed only low expression almost below the detection limit. This transcription factor is dependent on environmental conditions, such as oxygen, signaling pathways (e.g. cAMP/PKA) and biofilm maturity (69). The expression pattern suggests that polymer-dependent surface signals primarily modulate the early adhesion response, while hyphae- and biofilm-specific signaling pathways are only weakly activated on these abiotic materials.

The moderate positive correlation between surface roughness and *ALS1* expression may be explained by the increased number of adhesion sites provided by rough surfaces, thereby promoting adhesion-related genes. In contrast, the negative correlation between surface polarity and *HWP1* as well as *EFG1* expression suggests that more polar surfaces may inhibit morphological transition. However, given the moderate strength of these correlations, additional factors are likely to contribute and further analyses are necessary.

Quantitative CLSM analyses complemented the molecular biological findings: The surface coverage of *C. albicans* was generally higher on PTFE than on PVC, with rough PVC surfaces covering a smaller covered area than smooth ones. The increased *ALS1* transcription on PTFE is associated with higher adhesion forces and greater cell binding, which explains the stronger initial adhesion and greater surface coverage. On PVC, however, *ALS1* induction was less pronounced, resulting in reduced initial adhesion and smaller biofilm areas.

Differences in biofilm height can be explained primarily by physical retention and microstructure: rougher PVC surfaces provided more niches for cell stacking and biofilm formation, consistent with observations that rough surfaces generally offer more adhesion opportunities (70). In contrast, despite high surface coverage, PTFE tended to form flat, monolayer-like biofilms. The low expression of HWP1 and *EFG1* supports this interpretation, as these genes are associated with hyphae formation and biofilm-specific developmental stages. Overall, the biofilms on both materials grow predominantly in the yeast state, with

the architecture (area coverage vs. height) being determined by the combination of surface chemistry, topography and biological developmental stage.

In summary, the results showed that polymer-dependent surfaces primarily modulate gene expression associated with the early adhesion stages of *C. albicans*. Higher *ALS1* values on PTFE promote stronger initial adhesion and larger biofilm areas. The low expression of *HWP1* and *EFG1* explains the lack of hyphae formation and flatter biofilm structure on both materials, especially PTFE. This underscores that material chemistry and microstructure not only influence adhesion forces on the level of surface molecules, but also influence molecular gene expression and by this early colonization and biofilm architecture of *C. albicans*.

Conclusion

In summary, the surface properties of polymeric materials significantly influenced the molecular adhesion of *C. albicans*. Force spectroscopy showed that cell-substrate interactions depend on both surface chemistry and microstructure, with a strong correlation found with roughness and surface free energy. High surface roughness resulted in increased adhesion forces, a larger number of contact points, and shorter detachment distances. In contrast, high surface energy was associated with lower adhesion forces, fewer contact points, and longer detachment distances. Pretreatment with artificial saliva altered these relationships. This strong influence on the initial adhesion also caused changes in cellular gene expression. Molecular biological analyses suggested that polymer-dependent signals primarily control the early adhesion response, while hyphae- and biofilm-specific signaling pathways are only weakly activated.

Despite the insights gained, the results must be interpreted in the context of methodological limitations of the *in vitro* experimental design. Although the use of a single reference strain of *C. albicans* ensures high reproducibility, it does not reflect the genetic and phenotypic diversity of clinical isolates. In addition, complex *in vivo* factors such as host immune responses, dynamic mechanical conditions, and microbial interactions are not taken into account. Likewise, the artificial saliva solution used enables controlled and reproducible conditions, but only partially reflects the natural oral environment. Future studies should therefore validate the results presented using multispecies biofilm models and human saliva samples to transfer the significant correlations of polymer surface properties and the molecular *Candida* response to real dental prostheses.

Declarations

Acknowledgements

Not applicable.

Author contributions

S.T. contributed to the experimental design, data acquisition and analysis, and drafted the original manuscript. L.B. prepared and characterized the test specimens (excluding saliva-related experiments), while S.T. conducted surface wettability measurements in the presence of saliva and performed microbiological investigations. S.H. and N.K. secured funding for the study, oversaw its progress, contributed to its conception, and provided critical feedback on the manuscript. M.S. and K.D.-N. concepted and supervised the study and contributed to revising the manuscript. All authors read and approved the final manuscript.

Funding

This work was funded by the Deutsche Forschungsgemeinschaft (DFG, German Research Foundation, grant number 470769735).

Data availability

The datasets used and/or analyzed during the current study are available from the corresponding author on reasonable request.

Compliance with ethical standards

Conflict of interest

The authors declare no competing interests.

Ethics approval and consent to participate

Not applicable.

Consent for publication

Not applicable.

References

1. Mallya S, Mallya S (2019) Candida and Oral Candidosis—A Review. J Health Allied Sci NU April 09(02):39–44. 10.1055/s-0039-1695651
2. Kaitlin F, Mitchell R, Zarnowski H, Sanchez JA, Edward EL, Reinicke JE, Nett, Aaron P (2015) Mitchell and David R. Andes. Community participation in biofilm matrix assembly and function. 112(31):4092–4097 (6 pages)
3. Gunaratnam G, Dudek J, Jung P, Becker SL, Jacobs K, Bischoff M (2021) u. a. Quantification of the Adhesion Strength of Candida albicans to Tooth Enamel. Microorganisms 25 Oktober 9(11):2213. 10.3390/microorganisms9112213

4. Massey J, Zarnowski R, Andes D (2023) Role of the extracellular matrix in *Candida* biofilm antifungal resistance. FEMS Microbiol Rev 1 November 47(6):fuad059. 10.1093/femsre/fuad059
5. Gad MM, Fouda SM (2020) Current perspectives and the future of Candida albicans-associated denture stomatitis treatment. Dent Med Probl 31 März 57(1):95–102. 10.17219/dmp/112861
6. Gendreau L, Loewy ZG (2011) Epidemiology and Etiology of Denture Stomatitis. J Prosthodont Juni 20(4):251–260. 10.1111/j.1532-849X.2011.00698.x
7. Nett JE, Marchillo K, Spiegel CA, Andes DR (2010) Development and Validation of an *In Vivo Candida albicans* Biofilm Denture Model. Infect Immun. September ;78(9):3650–9. 10.1128/IAI.00480-10
8. Cao Z, Sun X, Yeh CK, Sun Y (2010) Rechargeable Infection-responsive Antifungal Denture Materials. J Dent Res Dezember 89(12):1517–1521. 10.1177/0022034510379604
9. Delaloye J, Calandra T (2014) Invasive candidiasis as a cause of sepsis in the critically ill patient. Virulence Januar 5(1):161–169. 10.4161/viru.26187
10. Dekkers BGJ, Veringa A, Marriott DJE, Boonstra JM, Van Der Elst KCM, Doukas FF (2018) u. a. Invasive Candidiasis in the Elderly: Considerations for Drug Therapy. Drugs Aging September 35(9):781–789. 10.1007/s40266-018-0576-9
11. Brose L, Tamjidtash S, Doll-Nikutta K, Stiesch M, Kommerein N, Hahnel S Influence of roughness and surface free energy on adhesion and biofilm formation of Candida albicans to polymeric materials [Internet]. In Review; 2026 [zitiert 20. April 2026]. Verfügbar unter: https://www.researchsquare.com/article/rs-8953001/v1 10.21203/rs.3.rs-8953001/v1
12. Nobile CJ, Schneider HA, Nett JE, Sheppard DC, Filler SG, Andes DR (2008) u. a. Complementary Adhesin Function in C. albicans Biofilm Formation. Curr Biol Juli 18(14):1017–1024. 10.1016/j.cub.2008.06.034
13. Schena NC, Baker KM, Stark AA, Thomas DP, Cleary IA (Juli 2023) Constitutive ALS3 expression in Candida albicans enhances adhesion and biofilm formation of efg1, but not cph1 mutant strains. Hwang G, Herausgeber. PLOS ONE. 13. 18(7):e0286547. 10.1371/journal.pone.0286547
14. Holmes AR, Bandara BMK, Cannon RD (2002) Saliva Promotes Candida albicans Adherence to Human Epithelial Cells. J Dent Res Januar 81(1):28–32. 10.1177/002203450208100107
15. Holmes AR, Bandara BMK, Cannon RD (2002) Saliva Promotes Candida albicans Adherence to Human Epithelial Cells. J Dent Res Januar 81(1):28–32. 10.1177/002203450208100107
16. Atriwal T, Azeem K, Husain FM, Hussain A, Khan MN, Alajmi MF (2021) u. a. Mechanistic Understanding of Candida albicans Biofilm Formation and Approaches for Its Inhibition. Front Microbiol 30 April 12:638609. 10.3389/fmicb.2021.638609
17. Atriwal T, Azeem K, Husain FM, Hussain A, Khan MN, Alajmi MF (2021) u. a. Mechanistic Understanding of Candida albicans Biofilm Formation and Approaches for Its Inhibition. Front Microbiol 30 April 12:638609. 10.3389/fmicb.2021.638609
18. Mouhat M, Moorehead R, Murdoch C (2020) *In vitro Candida albicans* biofilm formation on different titanium surface topographies. Biomater Investig Dent 1 Januar 7(1):146–157. 10.1080/26415275.2020.1829489

19. Seabra CL, Botelho CM, Oliveira ACN, Henriques M. Influence of Saliva and Mucin on the Adhesion of *Candida* Oral Clinical Isolates. J Encapsulation Adsorpt Sci. 2015;05(04):217–27. doi:10.4236/jeas.2015.54018
20. Cabanillas B, Mallma-Medina A, Petkova-Gueorguieva M, Alvitez-Temoche D, Mendoza R, Mayta-Tovalino F (2021) Influence of the Surface Energy of Different Brands of Polymethyl Methacrylate on the Adherence of Candida albicans: An In Vitro Study. J Int Soc Prev Community Dent Januar 11(1):6–12. 10.4103/jispcd.JISPCD_291_20
21. Aguayo S, Marshall H, Pratten J, Bradshaw D, Brown JS, Porter SR (2017) u. a. Early Adhesion of *Candida albicans* onto Dental Acrylic Surfaces. J Dent Res Juli 96(8):917–923. 10.1177/0022034517706354
22. Kurtulmus H, Kumbuloglu O, Özcan M, Ozdemir G, Vural C (2010) Candida albicans adherence on silicone elastomers: Effect of polymerisation duration and exposure to simulated saliva and nasal secretion. Dent Mater Januar 26(1):76–82. 10.1016/j.dental.2009.09.001
23. Taubenberger AV, Hutmacher DW, Muller DJ (2014) Single-Cell Force Spectroscopy, an Emerging Tool to Quantify Cell Adhesion to Biomaterials. Tissue Eng Part B Rev Februar 20(1):40–55. 10.1089/ten.teb.2013.0125
24. Aguayo S, Donos N, Spratt D, Bozec L (2015) Single-bacterium nanomechanics in biomedicine: unravelling the dynamics of bacterial cells. Nanatechnol 13 Februar 26(6):062001. 10.1088/0957-4484/26/6/062001
25. Beaussart A, El-Kirat-Chatel S, Sullan RMA, Alsteens D, Herman P, Derclaye S (2014) u. a. Quantifying the forces guiding microbial cell adhesion using single-cell force spectroscopy. Nat Protoc Mai 9(5):1049–1055. 10.1038/nprot.2014.066
26. Qiu Y, Chien C, Maroulis B, Bei J, Gaitas A, Gong B (2022) Extending applications of AFM to fluidic AFM in single living cell studies. J Cell Physiol August 237(8):3222–3238. 10.1002/jcp.30809
27. Li M, Liu L, Zambelli T (2022) FluidFM for single-cell biophysics. Nano Res Februar 15(2):773–786. 10.1007/s12274-021-3573-y
28. Owens DK, Wendt RC (1969) Estimation of the surface free energy of polymers. J Appl Polym Sci August 13(8):1741–1747. 10.1002/app.1969.070130815
29. Hahnel S Die Eignung von Proteinmischungen als Speichelersatz für die bakterielle in vitro Adhäsion. 2007. Located at: Regensburg: Universität Regensburg: Medizinische Fakultät-Zahnmedizin
30. Hahnel S, Rosentritt M, Handel G, Bürgers R (2008) Influence of saliva substitute films on initial Streptococcus mutans adhesion to enamel and dental substrata. Dezember
31. Hahnel S, Rosentritt M, Handel G, Bürgers R (2009) Surface characterization of dental ceramics and initial streptococcal adhesion in vitro. Dent Mater J August
32. Ehrenfeld ML (2013) Untersuchungen zur Adhäsion von oralen Streptokokken an zahnärztliche Werkstoffe in Abhängigkeit von der Auswertmethodik in vitro. Medizinische Fakultät-Zahnmedizin, Universität Regensburg

33. Birgit Verena Wislsperger BVW (2012) Untersuchungen zur initialen Biofilmbildung von koaggregierenden oralen Keimen an zahnaerztlichen Werkstoffen in vitro. Regensburg. [Regensburg, Medizinische Fakultät - Zahnmedizin]: Universität Regensburg
34. Doll-Nikutta K, Winkel A, Yang I, Grote AJ, Meier N, Habib M (2022) u. a. Adhesion Forces of Oral Bacteria to Titanium and the Correlation with Biophysical Cellular Characteristics. Bioeng 17 Oktober 9(10):567. 10.3390/bioengineering9100567
35. Schneider CA, Rasband WS, Eliceiri KW (2012) NIH Image to ImageJ: 25 years of image analysis. Nat Methods Juli 9(7):671–675. 10.1038/nmeth.2089
36. Derkacz D, Krasowska A (2023) Alterations in the Level of Ergosterol in Candida albicans' Plasma Membrane Correspond with Changes in Virulence and Result in Triggering Diversed Inflammatory Response. Int J Mol Sci 16 Februar 24(4):3966. 10.3390/ijms24043966
37. Bozec L, Donos N, Spratt D, Aguayo S (2016) Probing the nanoadhesion of Streptococcus sanguinis to titanium implant surfaces by atomic force microscopy. Int J Nanomed April 1443. 10.2147/IJN.S100768
38. Doll-Nikutta K, Winkel A, Yang I, Grote AJ, Meier N, Habib M (2022) u. a. Adhesion Forces of Oral Bacteria to Titanium and the Correlation with Biophysical Cellular Characteristics. Bioeng 17 Oktober 9(10):567. 10.3390/bioengineering9100567
39. Chen Y, Busscher HJ, Van Der Mei HC, Norde W (2011) Statistical Analysis of Long- and Short-Range Forces Involved in Bacterial Adhesion to Substratum Surfaces as Measured Using Atomic Force Microscopy. Appl Environ Microbiol August 77(15):5065–5070. 10.1128/AEM.00502-11
40. Aguayo S, Donos N, Spratt D, Bozec L (2015) Nanoadhesion of *Staphylococcus aureus* onto Titanium Implant Surfaces. J Dent Res August 94(8):1078–1084. 10.1177/0022034515591485
41. Helenius J, Heisenberg CP, Gaub HE, Muller DJ (2008) Single-cell force spectroscopy. J Cell Sci 1 Juni 121(11):1785–1791. 10.1242/jcs.030999
42. Alhajj MN, Halboub E, Yacob N, Al-Maweri SA, Ahmad SF (2024) Celebić A, u. a. Adhesion of Candida Albicans to digital versus conventional acrylic resins: a systematic review and meta-analysis. BMC Oral Health 4 März 24(1):303. 10.1186/s12903-024-04083-2
43. Ranc H, Elkhyat A, Servais C, Mac-Mary S, Launay B, Humbert P (2006) Friction coefficient and wettability of oral mucosal tissue: Changes induced by a salivary layer. Colloids Surf Physicochem Eng Asp März 276(1–3):155–161. 10.1016/j.colsurfa.2005.10.033
44. Sipahi C, Anil N, Bayramli E (2001) The effect of acquired salivary pellicle on the surface free energy and wettability of different denture base materials. J Dent Mai 29(3):197–204. 10.1016/S0300-5712(01)00011-2
45. Hannig C, Hannig M, Attin T (2005) Enzymes in the acquired enamel pellicle. Eur J Oral Sci Februar 113(1):2–13. 10.1111/j.1600-0722.2004.00180.x
46. Meder F, Kaur S, Treccani L, Rezwan K (2013) Controlling Mixed-Protein Adsorption Layers on Colloidal Alumina Particles by Tailoring Carboxyl and Hydroxyl Surface Group Densities. Langmuir 8 Oktober 29(40):12502–12510. 10.1021/la402093j

47. Meder F, Kaur S, Treccani L, Rezwan K (2013) Controlling Mixed-Protein Adsorption Layers on Colloidal Alumina Particles by Tailoring Carboxyl and Hydroxyl Surface Group Densities. Langmuir 8 Oktober 29(40):12502–12510. 10.1021/la402093j
48. Riivari S, Areid N, Närvä E, Willberg J, Närhi T (2024) Saliva exposure reduces gingival keratinocyte growth on TiO2-coated titanium. J Mater Sci Mater Med 18 April 35(1):25. 10.1007/s10856-024-06792-0
49. Potthoff E, Ossola D, Zambelli T, Vorholt JA (2015) Bacterial adhesion force quantification by fluidic force microscopy. Nanoscale 7(9):4070–4079. 10.1039/C4NR06495J
50. Gunaratnam G, Leisering R, Wieland B, Dudek J, Miosge N, Becker SL (2024) u. a. Characterization of a unique attachment organelle: Single-cell force spectroscopy of *Giardia duodenalis* trophozoites. Nanoscale 16(14):7145–7153. 10.1039/D4NR00122B
51. Gunaratnam G, Dudek J, Jung P, Becker SL, Jacobs K, Bischoff M (2021) u. a. Quantification of the Adhesion Strength of Candida albicans to Tooth Enamel. Microorganisms 25 Oktober 9(11):2213. 10.3390/microorganisms9112213
52. Alsteens D, Beaussart A, Derclaye S, El-Kirat-Chatel S, Park HR, Lipke PN (2013) u. a. Single-cell force spectroscopy of Als-mediated fungal adhesion. Anal Methods 5(15):3657. 10.1039/c3ay40473k
53. Beaussart A, Herman P, El-Kirat-Chatel S, Lipke PN, Kucharíková S, Van Dijck P (2013) u. a. Single-cell force spectroscopy of the medically important Staphylococcus epidermidis–Candida albicans interaction. Nanoscale 5(22):10894. 10.1039/c3nr03272h
54. Awassa J, Soulé S, Cornu D, Ruby C, El-Kirat-Chatel S (2024) Understanding the nanoscale adhesion forces between the fungal pathogen *Candida albicans* and antimicrobial zinc-based layered double hydroxides using single-cell and single-particle force spectroscopy. Nanoscale 16(10):5383–5394. 10.1039/D3NR06027F
55. Mei L, Ren Y, Busscher HJ, Chen Y, Van Der Mei HC (2009) Poisson Analysis of Streptococcal Bond-strengthening on Saliva-coated Enamel. J Dent Res September 88(9):841–845. 10.1177/0022034509342523
56. Mei L, Busscher HJ, Van Der Mei HC, Ren Y (2011) Influence of surface roughness on streptococcal adhesion forces to composite resins. Dent Mater August 27(8):770–778. 10.1016/j.dental.2011.03.017
57. Doll K, Yang I, Fadeeva E, Kommerein N, Szafrański SP (2019) Bei Der Wieden G, u. a. Liquid-Infused Structured Titanium Surfaces: Antiadhesive Mechanism to Repel *Streptococcus oralis* Biofilms. ACS Appl Mater Interfaces 3 Juli 11(26):23026–23038. 10.1021/acsami.9b06817
58. Hermansson M (1999) The DLVO theory in microbial adhesion. Colloids Surf B Biointerfaces August 14(1–4):105–119. 10.1016/S0927-7765(99)00029-6
59. Potthoff E, Guillaume-Gentil O, Ossola D, Polesel-Maris J, LeibundGut-Landmann S, Zambelli T (2012) u. a. Rapid and Serial Quantification of Adhesion Forces of Yeast and Mammalian Cells. Dague E, Herausgeber. PLoS ONE 20 Dezember 7(12):e52712. 10.1371/journal.pone.0052712

60. Dehullu J, Valotteau C, Herman-Bausier P, Garcia-Sherman M, Mittelviefhaus M, Vorholt JA (2019) u. a. Fluidic Force Microscopy Demonstrates That Homophilic Adhesion by *Candida albicans* Als Proteins Is Mediated by Amyloid Bonds between Cells. Nano Lett 12 Juni 19(6):3846–3853. 10.1021/acs.nanolett.9b01010
61. Lipke PN, Klotz SA, Dufrene YF, Jackson DN, Garcia-Sherman MC (2018) Amyloid-Like β-Aggregates as Force-Sensitive Switches in Fungal Biofilms and Infections. Microbiol Mol Biol Rev März 82(1):e00035–e00017. 10.1128/MMBR.00035-17
62. El-Kirat-Chatel S, Beaussart A, Derclaye S, Alsteens D, Kucharíková S, Van Dijck (2015) P, u. a. Force Nanoscopy of Hydrophobic Interactions in the Fungal Pathogen *Candida glabrata*. ACS Nano 24 Februar 9(2):1648–1655. 10.1021/nn506370f
63. Maikranz E, Spengler C, Thewes N, Thewes A, Nolle F, Jung P (2020) u. a. Different binding mechanisms of *Staphylococcus aureus* to hydrophobic and hydrophilic surfaces. Nanoscale 12(37):19267–19275. 10.1039/D0NR03134H
64. Zhang Y, Zhao Y, Qian Z, Wang Q, Yalikun N, Jiang H (2025) u. a. A hydrophilic/hydrophobic switch on polymer surface triggered by calcite towards separation of hazardous PVC from plastic mixtures. J Hazard Mater Februar 483:136667. 10.1016/j.jhazmat.2024.136667
65. Puerner C, Kukhaleishvili N, Thomson D, Schaub S, Noblin X, Seminara A (2020) u. a. Mechanical force-induced morphology changes in a human fungal pathogen. BMC Biol Dezember 18(1):122. 10.1186/s12915-020-00833-0
66. Lampin M, Warocquier-Cl□rout R, Legris C, Degrange M, Sigot-Luizard MF (1997) Correlation between substratum roughness and wettability, cell adhesion, and cell migration. J Biomed Mater Res Juli 36(1):99–108. 10.1002/(SICI)1097-4636::AID-JBM12>3.0.CO;2-E
67. Bu Y, Ma J, Bei J, Wang S (2019) Surface Modification of Aliphatic Polyester to Enhance Biocompatibility. Front Bioeng Biotechnol 3 Mai 7:98. 10.3389/fbioe.2019.00098
68. Majhy B, Priyadarshini P, Sen AK (2021) Effect of surface energy and roughness on cell adhesion and growth – facile surface modification for enhanced cell culture. RSC Adv 11(25):15467–15476. 10.1039/D1RA02402G
69. Stichternoth C, Ernst JF (2009) Hypoxic Adaptation by Efg1 Regulates Biofilm Formation by *Candida albicans*. Appl Environ Microbiol Juni 75(11):3663–3672. 10.1128/AEM.00098-09
70. Yalçın S, özel S, çamyar D (2025) bonabian E farboud. Candida albicans Impact on the Progression, Morphology, and Cellular Integrity of Biofilm Formation on the Surfaces of Implants; Current Knowledge and Future Perspectives. Int J Mol Cell Med Juli 14(2). 10.22088/IJMCM.BUMS.14.2.620

Figures

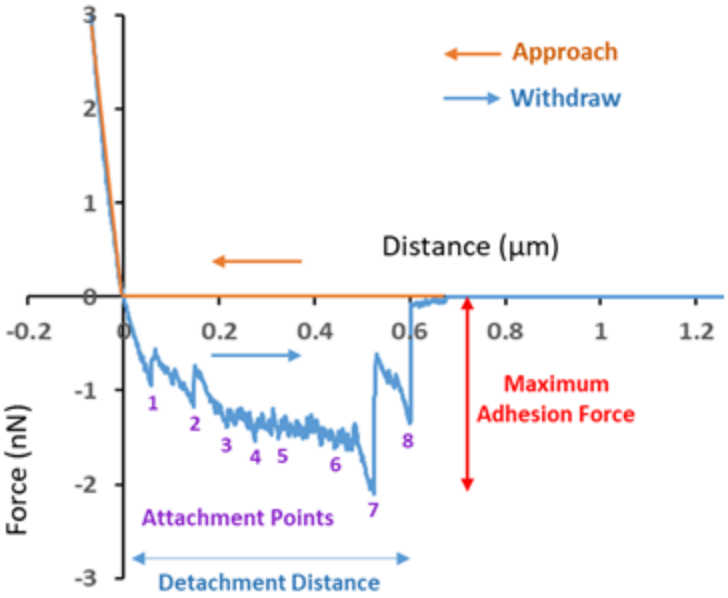


Figure 1

Schematic Depiction of Quantitative Parameters Derived from Force–Distance Curves in Single-Cell Force Spectroscopy. The orange curve represents the approach of *C. albicans* cells toward the surface, while the blue curve depicts its retraction.

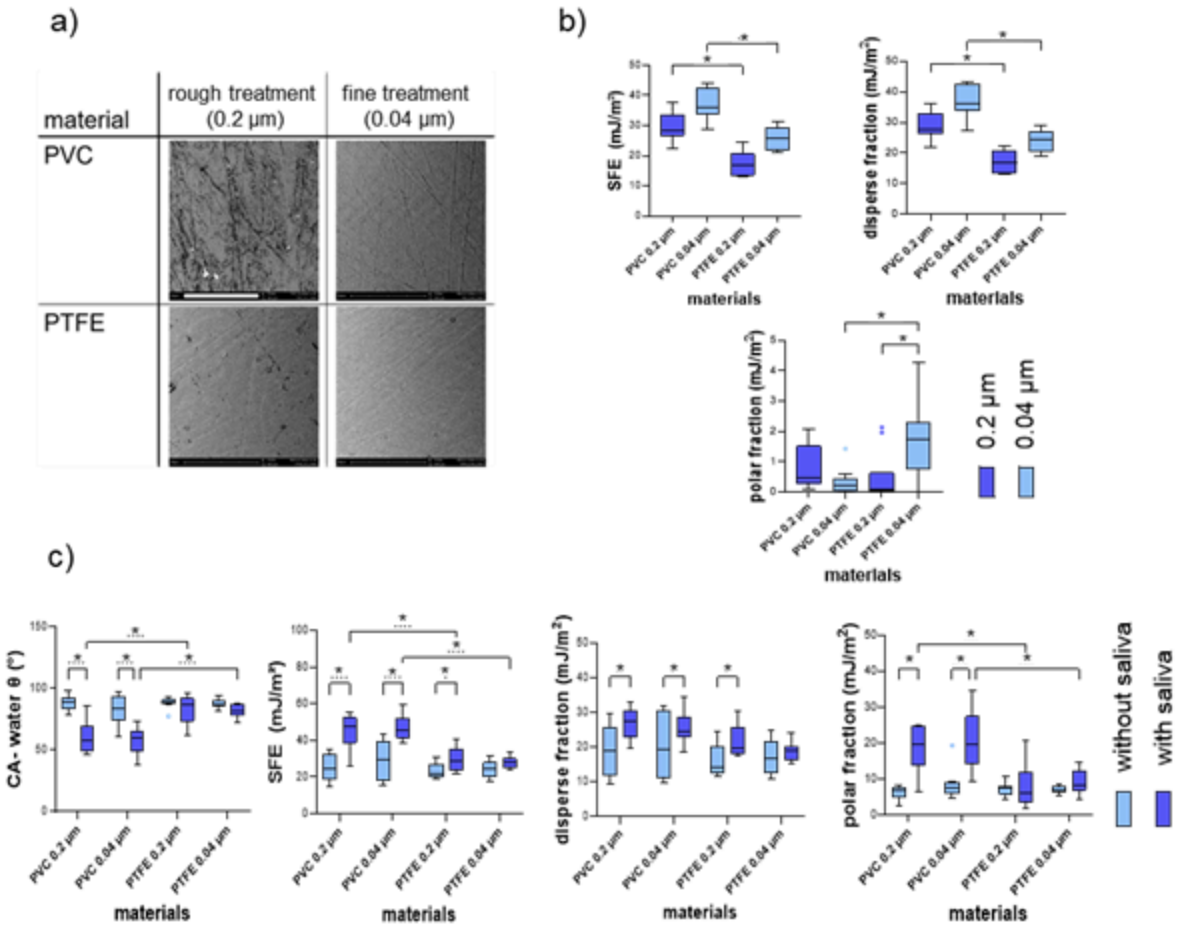


Figure 2

Quantitative analysis of the surface properties of standard polymer materials.

a) Representative SEM images (magnification 1500´) of PVC and PTFE following different surface treatments. Scale bar equals 80 µm for all images.

b) Tukey boxplots for water contact angle, surface free energy (SFE), and its dispersed and polar components of standard polymers after two different surface treatments without saliva coating.

c) Tukey boxplots of SFE and its dispersive and polar components following rough and fine surface treatments after saliva coating.

(N = 10; * indicates statistically significant differences with $p \leq 0.05$).

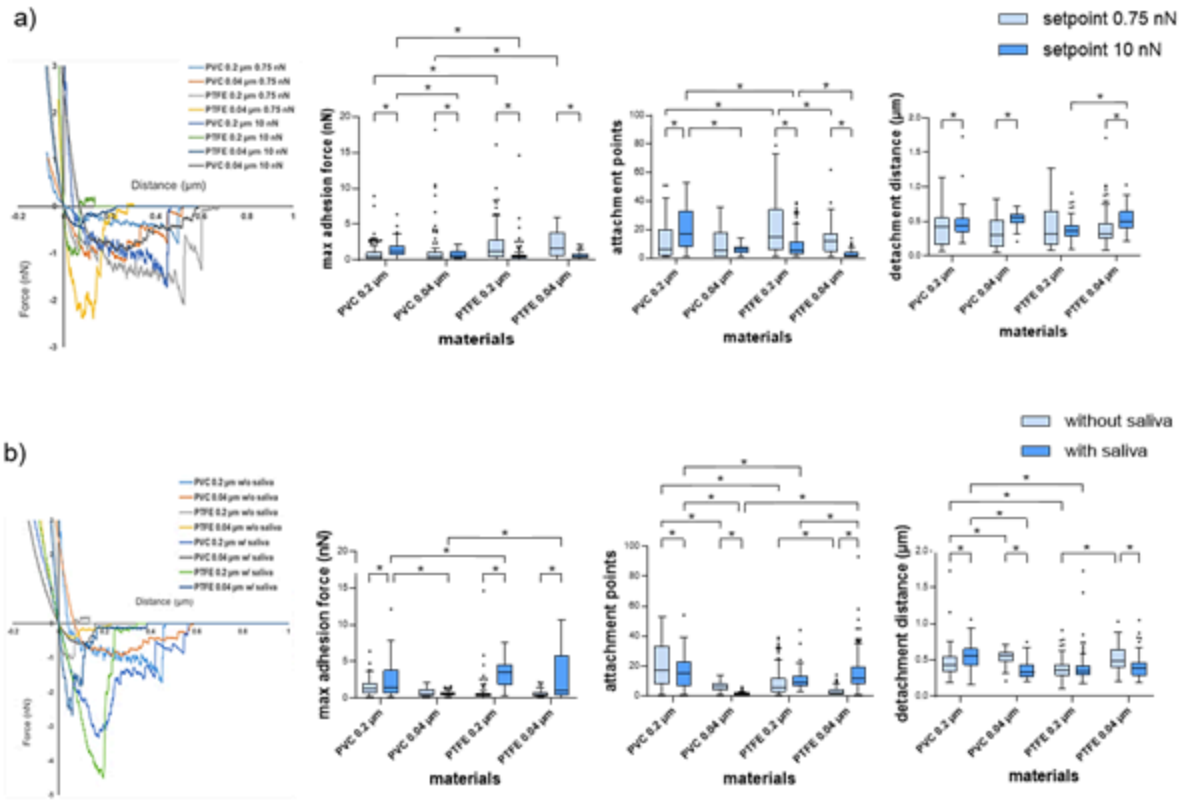


Figure 3

Adhesion forces of individual *C. albicans* cells on PVC and PTFE surfaces.

a) Exemplary force–distance curves on different surfaces with different contact forces and Tukey box plots of the resulting maximum adhesion forces, number of adhesion points, and detachment distance. The measurements were performed with an adhesion time of 2 seconds andwith contact forces of 0.75 nN and 10 nN (N = 63–201 after quality control).

b) Exemplary force–distance curves on different surfaces with and without saliva coating and Tukey box plots of the resulting maximum adhesion forces, number of adhesion points, and detachment distance. The measurements were performed with an adhesion time of 2 seconds and a contact force of 10 nN (N = 75–137 after quality control).

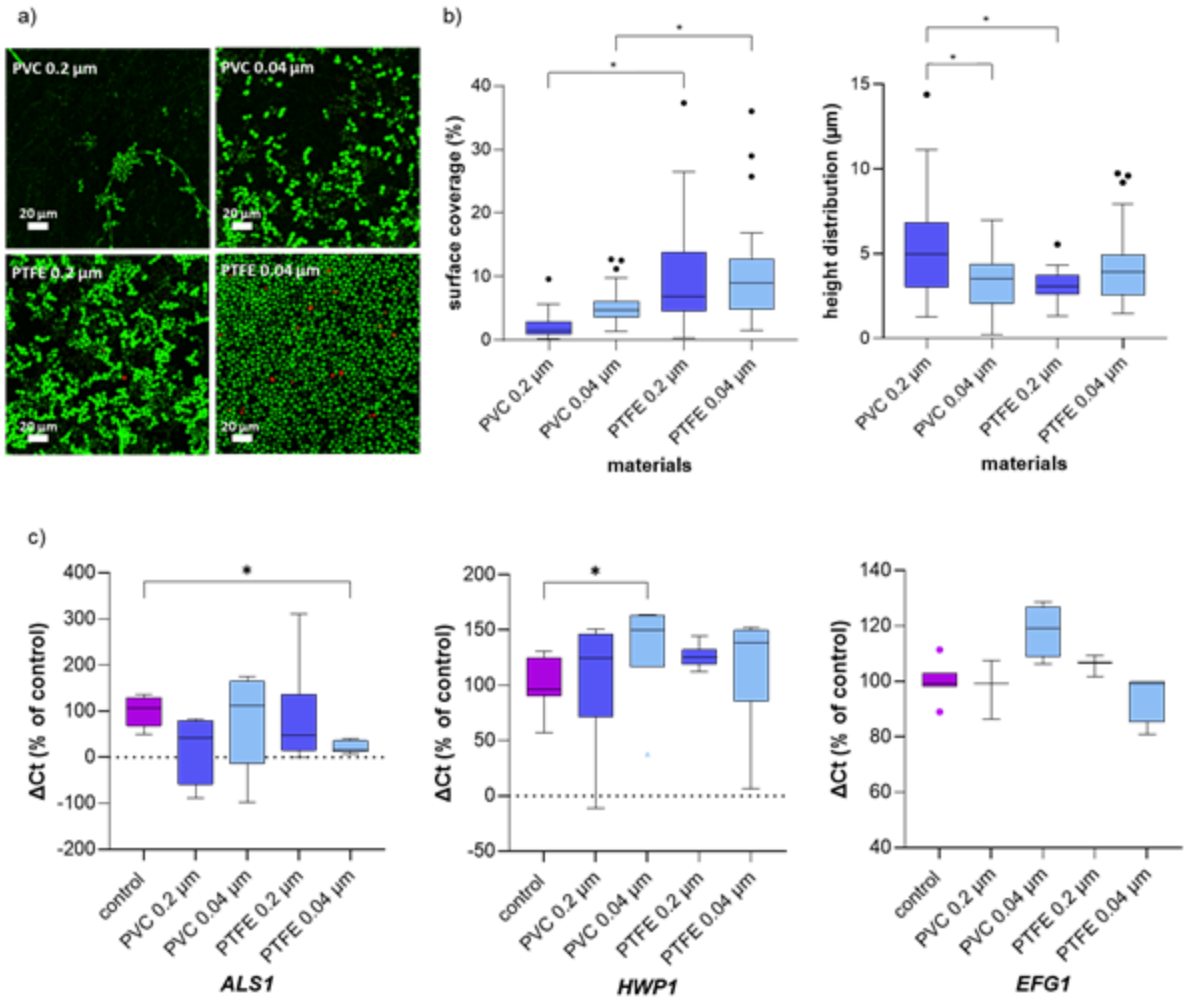


Figure 4

Gene expression in *C. albicans* biofilms on PVC and PTFE surfaces. a) Representative CLSM images of *C. albicans* biofilm formation on different polymeric materials (magnification 63x; white bar: 20 µm; Imaris X64). Green: vital cells; red: dead cells.

Biofilm parameters are displayed as Tukey boxplots of **b)** percent surface coverage and biofilm height on different material surfaces calculated with ImageJ (N > 37, * indicates statistically significant differences with $p \leq 0.05$).

c) Tukey box plots of ΔCt values of selected genes expressed in *C. albicans* biofilms on PVC and PTFE surfaces relative to the well plate control. Results were calculated in comarison to the housekeeping gene *ACT1* andexpressed relative to the well plate control (N = 6; * indicates statistically significant differences with $p \leq 0.05$).

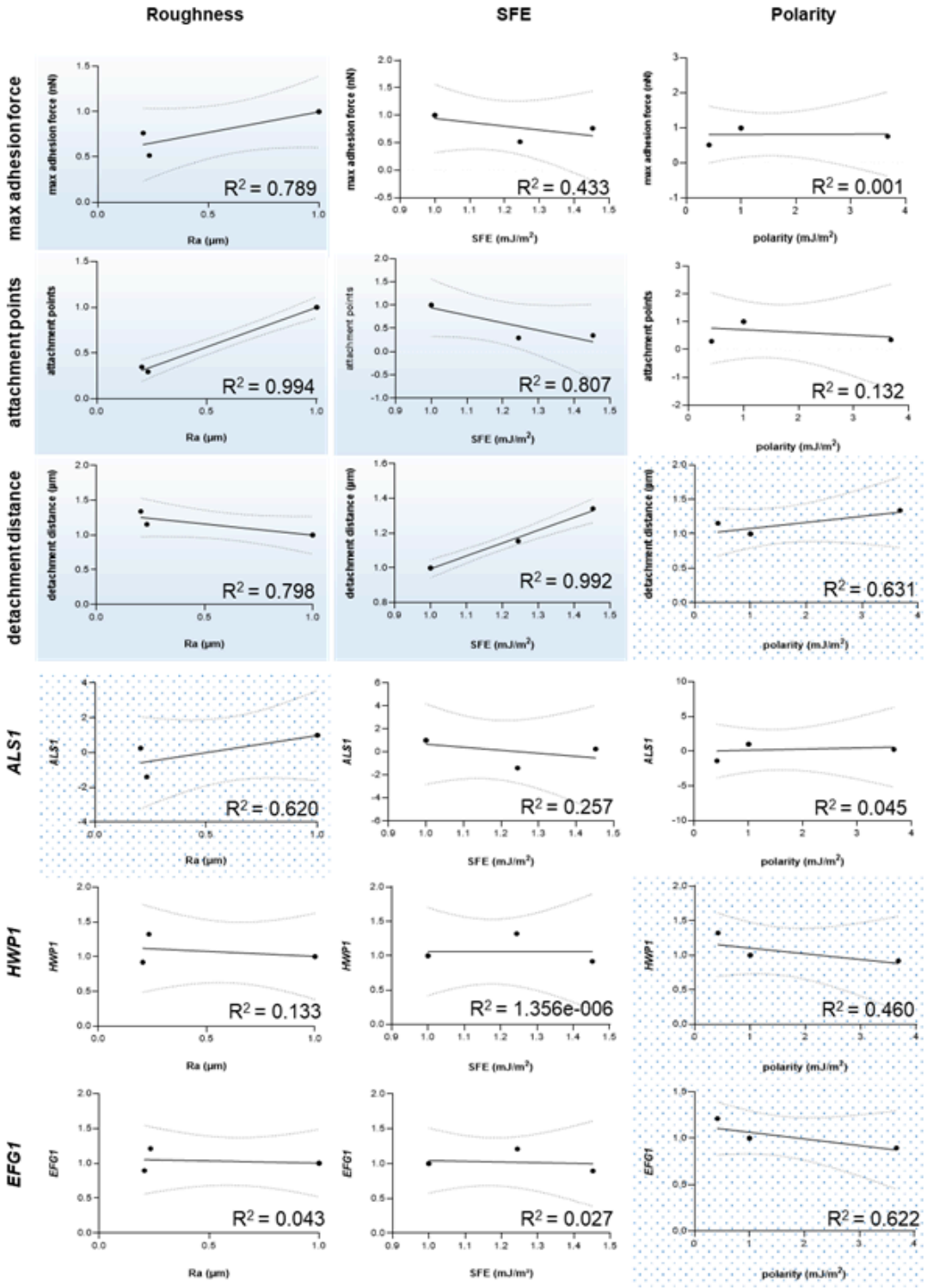


Figure 5

Linear regression between polymer surface parameters and molecular response of *C. albicans*. The values were normalized relative to the respective values of the rougher surface (0.2 µm). The linear regression line is shown with a 95% confidence interval, as is the corresponding correlation coefficient R^2. Correlations with a high correlation coefficient are highlighted in blue. Moderate correlations are indicated by dotted backgrounds.

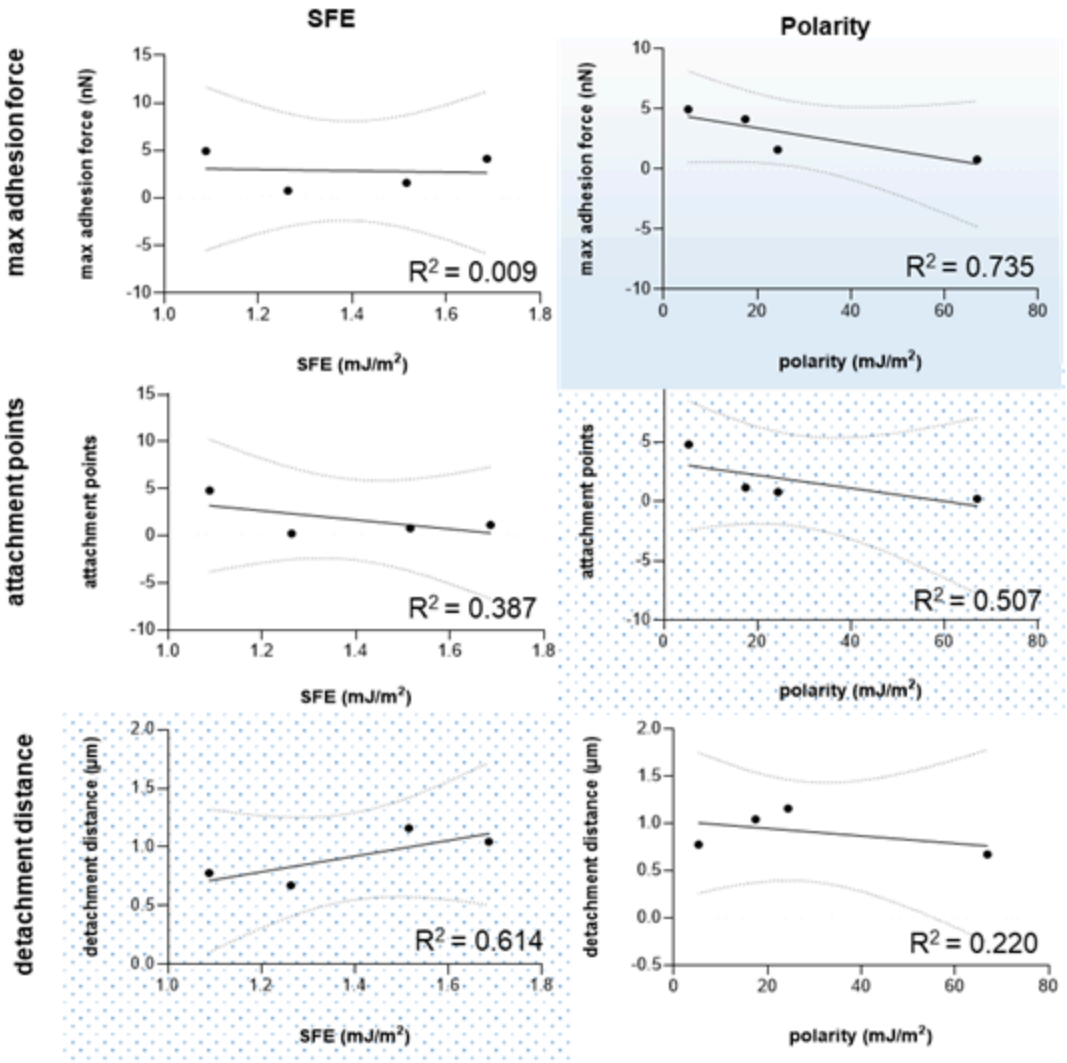


Figure 6

Linear regression between saliva treated polymer surface parameters and the adhesion force parameters of *C. albicans*. The values were normalized to the corresponding measurements obtained without saliva. The linear regression line is shown with a 95% confidence interval, along with the corresponding coefficient of determination (R^2). Correlations with high R^2 values are highlighted in blue. Moderate correlations are indicated by dotted backgrounds.

Supplementary Files

This is a list of supplementary files associated with this preprint. Click to download.

- supplement.png